Journal of Applied Polymer Science

Improving the toughness of epoxy with a reactive tetrablock copolymer containing maleic anhydride

Ren He, Xiaoli Zhan, Qinghua Zhang, Fengqiu Chen
College of Chemical and Biological Engineering, Zhejiang University, Hangzhou 310027, People's Republic of China
Correspondence to: Q. Zhang (E-mail: qhzhang@zju.edu.cn)

ABSTRACT: Reactive block copolymers (BCPs) provide a unique means for toughening epoxy thermosets because covalent linkages provide opportunities for greater improvement in the fracture toughness (K_{IC}). In this study, a tailored reactive tetrablock copolymer, poly[styrene-*alt*-(maleic anhydride)]-*block*-polystyrene-*block*-poly(*n*-butyl acrylate)-*block*-polystyrene, was incorporated into a diglycidyl ether of bisphenol A based epoxy resin. The results demonstrate the advantage of reactive BCP in finely tuning and controlling the structure of epoxy blends, even with 95 wt % epoxy-immiscible triblocks. The size of the dispersed phase was efficiently reduced to submicrometer level. The mechanical properties, such as K_{IC}, of these cured blends were investigated. The addition of 10 wt % reactive BCP into the epoxy resins led to considerable improvements in the toughness, imparting nearly a 70% increase in K_{IC}. The designed reactive tetrablock copolymer opened good prospects because of its potential novel applications in toughening modification of engineering polymer composites. © 2015 Wiley Periodicals, Inc. J. Appl. Polym. Sci. **2016**, *133*, 42826.

KEYWORDS: composites; copolymers; mechanical properties; structure–property relations; thermosets

Received 30 May 2015; accepted 10 August 2015
DOI: 10.1002/app.42826

INTRODUCTION

Epoxy resins have been widely applied as matrices of adhesives and structural materials because of their highly crosslinked nature. This feature also brings certain drawbacks, including brittleness and notch sensitivity.[1] To expand their applications, the toughening modification of epoxy resins has attracted researcher's attention for many years.[2–10] Recently, it has been demonstrated that the incorporation of block copolymers (BCPs) is much more efficient at toughening brittle epoxy thermosets.[11–19] Unlike oligomeric or core–shell rubber inclusions, BCPs are effective at low loadings without significant sacrifices of the modulus or glass-transition temperature (T_g) of the thermosets.[20] The main concept of BCPs in modifying epoxy blends is their miscibility in epoxy blends. To generate nanostructured thermosets, at least one epoxy-miscible block and one epoxy-immiscible block must be introduced into these BCPs.[16,19,21–26]

In the cases where the BCP does not have any segments miscible with the epoxy resin, it is essential to chemically modify one of the blocks to make it miscible with the epoxy resin.[8,19] Bates *et al.*[27] found that epoxy groups in the reactive BCPs poly(epoxy isoprene)-*block*-polybutadiene and poly(methyl acrylate-*co*-glycidyl methacrylate)-*block*-polyisoprene were able to react with the amine end groups of the hardener. These reactive BCPs could cure in the epoxy network without macrophase separation. To improve the compatibility between commercial elastomers and epoxy resins, the double bonds in polystyrene-*block*-poly(*n*-butyl acrylate)-*block*-polystyrene were epoxidized to be reactive; thus, long-range ordered nanostructures in epoxidized polystyrene-*block*-poly(*n*-butyl acrylate)-*block*-polystyrene/diglycidyl ether of bisphenol A (DGEBA) blends cured with 4,4′-diaminodiphenyl methane (DDM) were achieved.[28–30] In previous studies, the reactive groups introduced into the BCPs were not able to react with DGEBA or were randomly distributed.[18,27,31] This was because the most of commercial BCPs were prepared through anionic polymerization; this made it difficult, by definition, to introduce a wide variety of reactive groups on account of undesirable terminations.[27,31,32] In recent years, with the advances of controlled radical polymerization, reversible addition–fragmentation chain-transfer polymerization can be easily applied to the preparation of amphiphilic BCPs over a wide temperature range because of its functional group tolerance.[33,34] Through this method, a lot of innovative BCPs elastomers composed of soft and hard segments with interesting properties have been conveniently synthesized.

It has been reported that maleic anhydride containing copolymers improve the interfacial compatibility between epoxy-immiscible elastomers and the epoxy matrix.[35] In our prior work, the tetrablock copolymer poly[styrene-*alt*-(maleic anhydride)]-*block*-polystyrene-*block*-poly(*n*-butyl acrylate)-*block*-polystyrene (SMA–SBAS) was successfully obtained. However, the effect of the BCPs on the

Table I. Structure of the Synthesized Tetrablock Copolymer SMA_{5K}–PSt_{20K}–$PnBA_{40K}$–PSt_{20K}

After chain extension	SMA	SMA-PSt	SMA-PSt-PnBA	SMA-SBAS
Number-average molecular weight (g/mol)[a]	4,503	23,500	64,200	91,400
Polydispersity index[a]	1.18	1.09	2.68	3.04
wt %[b]	4.93	20.78	43.90	29.76

[a] Determined from a gel permeation chromatography analysis. The data were accumulative after chain extension.
[b] Calculated with data obtained from gel permeation chromatography measurements.

toughness modification has not yet been extensively explored, and the underlying toughening mechanism is not well understood.

In this study, the tailored reactive tetrablock copolymer SMA-SBAS was applied to the toughening of DGEBA/DDM epoxy thermosets. This article presents the effects of maleic anhydride as a reactive group in copolymers on the nanostructure and mechanical performance of thermosets. The morphologies of the blends were verified by optical clarity, transmission electron microscopy (TEM), and scanning electron microscopy (SEM) observations. The thermal and mechanical properties were investigated with dynamical mechanical thermal analysis by dynamic mechanical analysis (DMA) and fracture toughness (K_{IC}) measurements. The main emphasis of this research was the effects of the addition of reactive sites to the backbone on the improvement of the miscibility and structural and mechanical properties of multiblock copolymer thermoplastic elastomer modified epoxy thermosets.

EXPERIMENTAL

Materials

A tailor-made tetrablock copolymer, SMA–SBAS, was prepared, as described in literature.[36] The molecular structure of the tetrablock copolymer SMA_{5K}–PSt_{20K}–$PnBA_{40K}$–PSt_{20K} is shown in Table I and Scheme 1. The epoxy resin used in this study was DGEBA (E51, Shanghai Resin Production, epoxy value = 0.51 mol/100 g). DDM (97%, Aldrich) was used as a hardener. The amino hydrogen to epoxy stoichiometric ratio of one was selected for all of the systems. Tetrahydrofuran (99.9%, Aldrich) was used as a cosolvent to obtain homogeneous mixtures of high-molecular-weight BCP and DGEBA.

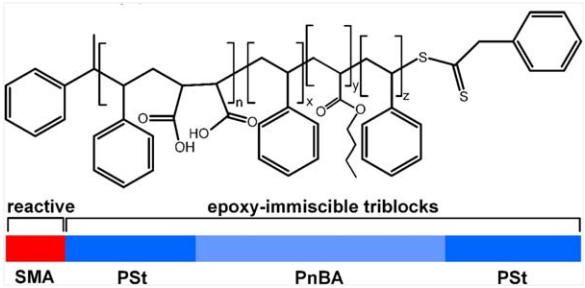

Scheme 1. Chemical structure of an SMA–SBAS tetrablock copolymer containing a reactive epoxy-miscible SMA block. [Color figure can be viewed in the online issue, which is available at wileyonlinelibrary.com.]

Preparation of the Reactive-BCP-Modified Thermosets

Tetrahydrofuran was used as cosolvent to facilitate the homogeneous mixing of the epoxy and BCP at room temperature. Once homogeneity was achieved, the mixture was heated to 90°C to completely remove the solvent. Then, a stoichiometric amount of the hardener DDM was added to the mixture and magnetically stirred until the hardener was completely dissolved. Uniform and bubble-free plaques were obtained through pouring of the mixture into a preheated mold and kept in a vacuum oven for 6 h. The blends were cured at 50°C for 2 h, 100°C for 3 h, and 130°C for 3 h in the oven and then slowly cooled down to room temperature. The absence of bubbles in the cured parallelepiped bars indicated that the solvent was removed.

Characterization

Fourier Transform Infrared (FTIR) Spectroscopy. To identify the reaction between the epoxy groups of DGEBA and the carboxyl groups of the BCP, FTIR measurements were performed on a Nicolet 5700 FTIR spectrometer with an OMNIC workstation. A blend of SMA–SBAS/DGEBA (40:60 w/w) was measured after several hours of stirring at 80°C to maximize the reaction between the carboxyl groups and epoxy groups. Samples were prepared as KBr pellets and scanned against a blank KBr pellet background at wave numbers ranging from 4000 to 400 cm^{-1} with resolution of 4.0 cm^{-1} through the accumulation of 256 scans.

Ultraviolet–Visible (UV–vis) Transmittance Spectra. The UV–vis transmittance spectra of the cured neat epoxy and SMA–SBAS modified epoxy parallelepiped bars (thickness = 4 mm) were obtained with a SpectraMax M2 in the range between 200 and 800 nm at 50 nm per step.

SEM. The morphology of the fractured surface of the epoxy/SMA–SBAS blends were measured with an FEI Sirion scanning electron microscope. The fractured samples were prepared after they were cooled in liquid N_2 and at room temperature and then coated with platinum by vapor deposition before observation.

TEM. The morphological characterization of the SMA–SBAS modified epoxy blends was analyzed by a JEOL JEM-1230L microscope with the application of an acceleration voltage of 120 kV. The ultrathin sections were prepared with a Leica Ultracut ultramicrotome at room temperature and collected on a copper grid.

DMA. The temperature dependences of the viscoelastic properties [storage modulus (G') and loss tangent (tan δ)] of the cured epoxy or cured blends were examined by a TA Q800

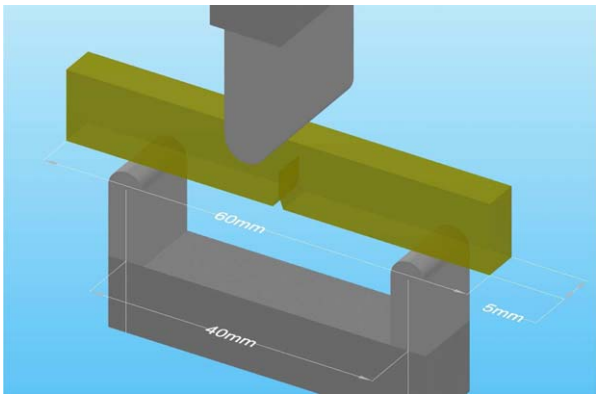

Scheme 2. Schematic of a specimen with the single-edge-notched three-point blending method. [Color figure can be viewed in the online issue, which is available at wileyonlinelibrary.com.]

instrument (TA Instruments). The dimensions of the specimens were 35.5 × 12 × 1.5 mm^3. The analysis was evaluated in torsion mode at a fixed frequency of 1 Hz and an amplitude of 15 μm and run from −140 to 200°C with temperature increases of 5°C/min. The peak in tan δ was considered to be T_g.

K_{IC} Measurements. K_{IC} measurements were performed according to the linear elastic fracture mechanics approach by a single-edge notched three-point blending (SENB) method according to ASTM D 5045-99. The dimensions of the parallelepiped specimens were 60 × 10 × 5 mm^3, as illustrated in Scheme 2. A Zwick/Roell Z020 universal material tester was used to perform the tests at a test speed of 10 mm/min (23°C). We carefully generated the cracks by first cutting a notch of approximately 4.5 mm using a diamond saw blade and then tapping a liquid-N_2-chilled fresh razor blade. The critical stress intensity factor was calculated by the averaging of values from at least five specimens.

RESULTS AND DISCUSSION

Miscibility of the SMA–SBAS Tetrablock Copolymer and Epoxy

It is known that polystyrene (PSt) and poly(*n*-butyl acrylate) (PnBA) are both epoxy-immiscible.[23,37] Therefore, it was important to assess the miscibility of the SMA segment with the epoxy resins. A model test was performed to evaluate the miscibility of the SMA segment in the cured epoxy. Here, 10 wt % of poly(styrene-*alt*-maleic acid) alternating copolymer (number-average molecular weight = 5000 g/mol) was added to the epoxy. The specimen of the SMA-modified epoxy blends was transparent [Figure 1(a)]. The fractured surface of the cured mixture was smooth [Figure 1(b)]. The model experiment indicated that the SMA alternating copolymer was miscible with the cured epoxy.

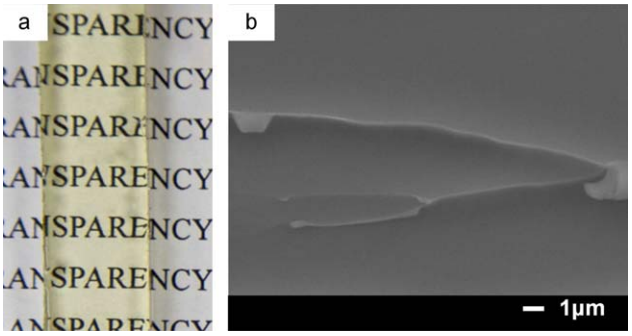

Figure 1. (a) Visual appearance of an epoxy blend modified by a 10 wt % SMA alternating copolymer. (b) SEM photographs of fracture surfaces of 10 wt % SMA modified DGEBA/DDM blends. [Color figure can be viewed in the online issue, which is available at wileyonlinelibrary.com.]

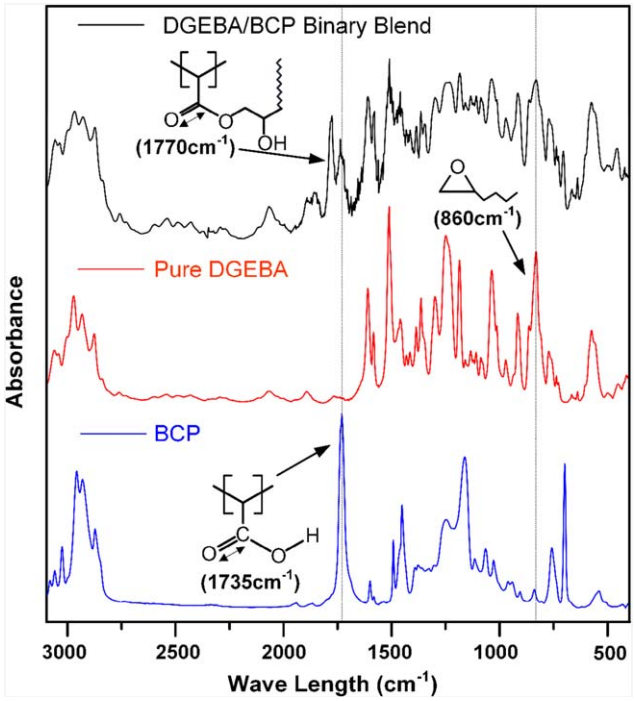

Figure 2. FT-IR spectra of BCP, SMA-SBAS, uncured pure DGEBA and uncured DGEBA/40 wt % BCP blends with no hardener. [Color figure can be viewed in the online issue, which is available at wileyonlinelibrary.com.]

FTIR measurements were taken to elucidate the reactivity of the remaining carboxylic acid in the tetrablock copolymer backbone. Figure 2 presents the FTIR spectra of the tetrablock copolymer SMA–SBAS, the pure DGEBA epoxy precursor, and DGEBA blended with 40 wt % SMA–SBAS. Compared to the pure DGEBA, the absorptions near 1735 cm^{-1} (carboxylic acid C═O stretching) and 860 cm^{-1} (epoxide C—O—C ring deformation) of the BCP/epoxy blend decreased. On the other hand, the absorption near 1770 cm^{-1} (ester C═O stretching) increased. These were clear signs of ester formation during the epoxy–carboxylic acid reaction and confirmed the reactivity between SMA–SBAS and DGEBA. In the blends, the existence of an absorption peak at 1735 cm^{-1} indicated that the carboxylic acid groups were not completely reacted. This was attributed to the combination effect of steric hindrance in the backbone and the limited reactivity of carboxylic acid diluted in the epoxy precursor. Indeed, the unreacted carboxylic acid had the opportunity to produce covalent bonds with the amine

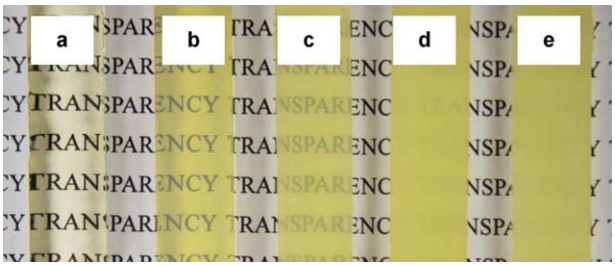

Figure 3. Transparency of the cured epoxy thermosets with the addition of different modifiers: (a) neat epoxy, (b) 5 wt % SMA–SBAS, (c) 10 wt % SMA–SBAS, (d) 15 wt % SMA–SBAS, and (e) 20 wt % SMA–SBAS. [Color figure can be viewed in the online issue, which is available at wileyonlinelibrary.com.]

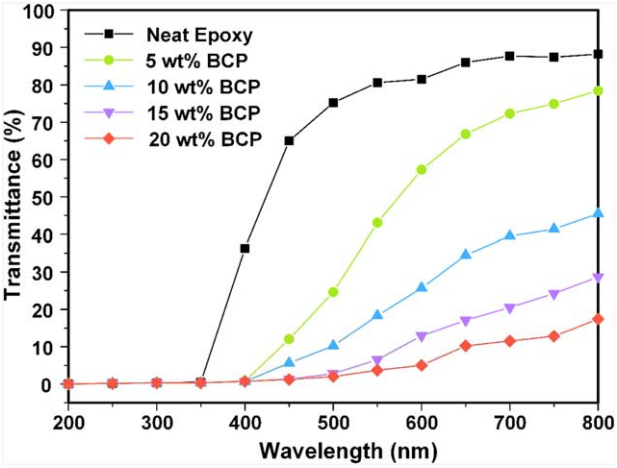

Figure 4. UV–vis transmittance spectra of the cured neat epoxy and SMA–SBAS BCP-modified blends. [Color figure can be viewed in the online issue, which is available at wileyonlinelibrary.com.]

hardeners during curing. A stronger interfacial adhesion between BCP inclusion and the epoxy matrix was obtained.

Optical Clarity

The transparency of the cured blends shown in Figure 3 demonstrates that the samples with a thickness of 4 mm gradually became opaque as more SMA–SBAS was added to the epoxy mixture. The carboxyl groups in BCP reacted with the epoxy in the DGEBA and [N—H] groups in the hardener DDM. This covalent bond should have maintained the phase structures of the blends. The epoxy blends modified by 10 wt % or less BCP were almost transparent [Figure 3(b,c)]. The cured blends containing 15 or 20 wt % BCP were opaque [Figure 3(d,e)]. This phenomenon suggested that the scale of inclusions was probably large enough to scatter visible light. The difference in the transparency indicated a difference in the scale of inclusions.

UV–vis measurements were carried out to study the optical transparency of the blends. Figure 4 shows the UV–vis transmittance spectra of the cured neat epoxy and all of the SMA–SBAS modified blends. The transmittance was strongly related to the thickness of the tested sample bars. The neat epoxy system showed the highest UV–vis transmittance. Increases in the light adsorption in both visible and UV ranges were observed with increases in the concentration of SMA–SBAS in the cured blends. This was in accordance with the transparency of the samples shown in Figure 3. The difference in the transparency indicated a difference in the scale of inclusions. SEM and TEM measurements were taken to further reveal the internal phase structures.

Phase Morphology of the Epoxy Blends

Figure 5 shows the SEM micrographs of the fractured surfaces of the SMA–SBAS modified epoxy blends chilled with liquid nitrogen. The neat epoxy thermosets exhibited a single phase, typically with a flat and smooth surface [Figure 5(a)]; this indicated a brittle material. The morphologies of the cured epoxy blends with the SMA–SBAS tetrablock copolymer showed rough fractured surfaces [Figure 5(b,c)]. Compared with the cured neat epoxy, these rough structures at low-temperature fracture faces were generated by the dispersion phase of low-T_g BCP in the SMA–SBAS modified epoxy blends. The 20 wt % SMA–SBAS modified cured blend [Figure 5(c)] was found to have cavities at the submicrometer level. For all of the samples, as the tetrablock copolymer SMA–SBAS contents increased from 5 to 20 wt %, the inclusion size increased.

TEM photographs of the cured blends in Figure 6 clearly reveal the difference in the size of the internal phase structures. The neat epoxy was uniform and homogeneous [Figure 6(a)]. The blends containing 5 wt % SMA–SBAS [Figure 6(b)] showed nanospheres around 100 nm dispersed in the epoxy resin matrix. The core of the spherical inclusions was epoxy-immiscible triblocks. A vesicle morphology was found in the 10 wt %

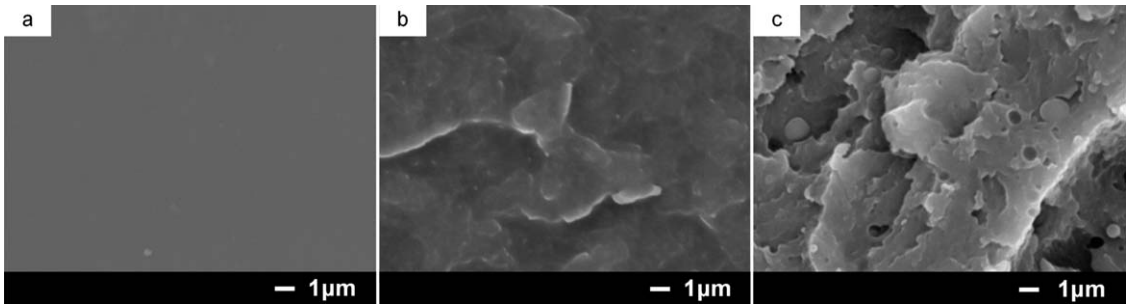

Figure 5. SEM photographs of the fracture surfaces of the DGEBA/DDM blends with BCPs at 10,000× magnification: (a) neat epoxy, (b) 10 wt % SMA–SBAS, and (c) 20 wt % SMA–SBAS.

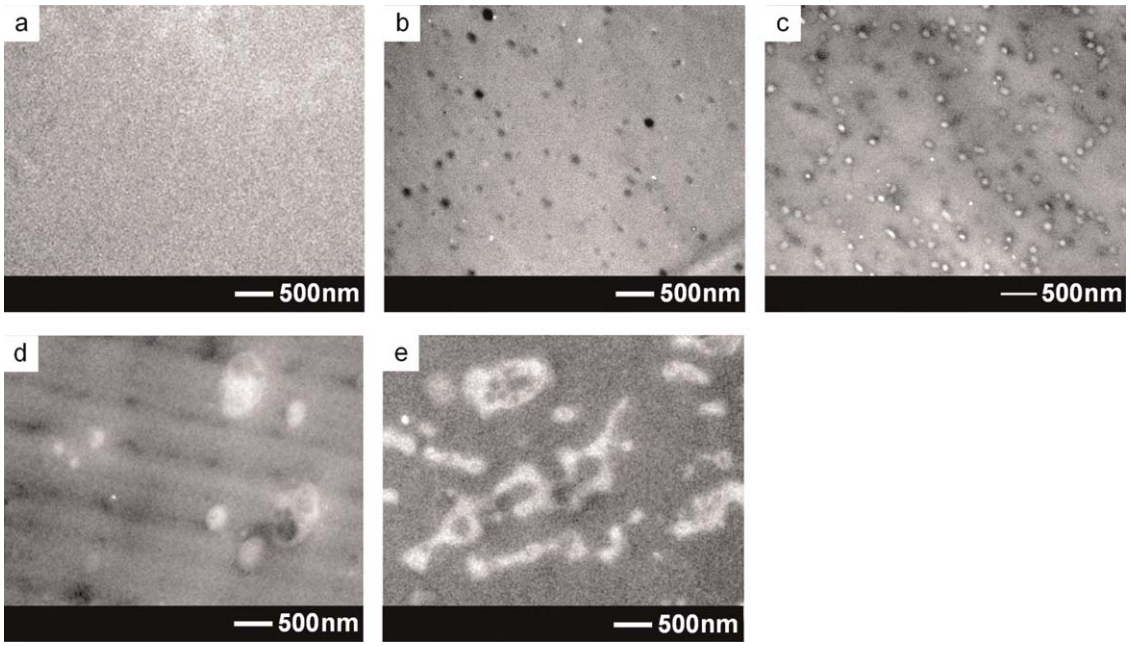

Figure 6. TEM photographs of the DGEBA/DDM blends with (a) 0, (b) 10, (c) 15, and (d) 20 wt % SMA–SBAS (scale bar = 500 nm.

SMA–SBAS modified epoxy, and the inner core was estimated to be DGEBA [Figure 6(c)]. With an increased loading of SMA–SBAS [15 wt %, Figure 6(d)], the cured blends were found to have complex structures. Nano–micro-inclusions were observed in the 20 wt % SMA–SBAS modified epoxy blends [Figure 6(e)]. TEM observations further confirmed the increased inclusion size at high SMA–SBAS concentrations; this revealed the detailed

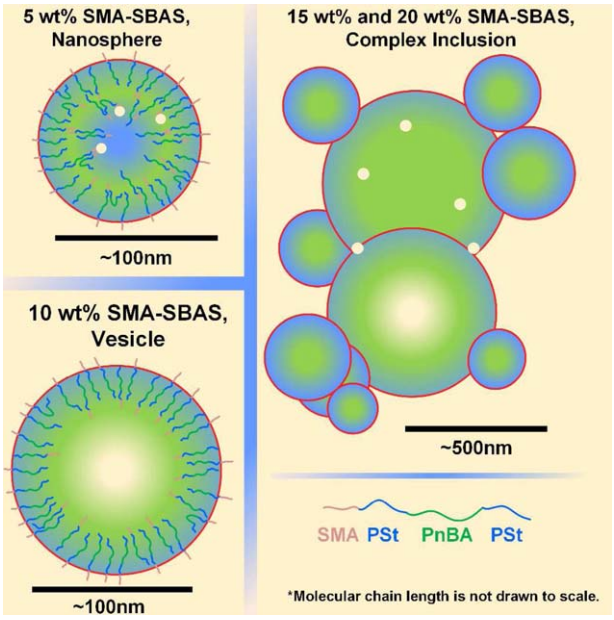

Scheme 3. Schematic illustration of the phase structures in the epoxy/SMA–SBAS blends. The SMA segment of the BCP was reactive with DGEBA/DDM, and the PSt–PnBA–PSt triblocks were immiscible with DGEBA/DDM. [Color figure can be viewed in the online issue, which is available at wileyonlinelibrary.com.]

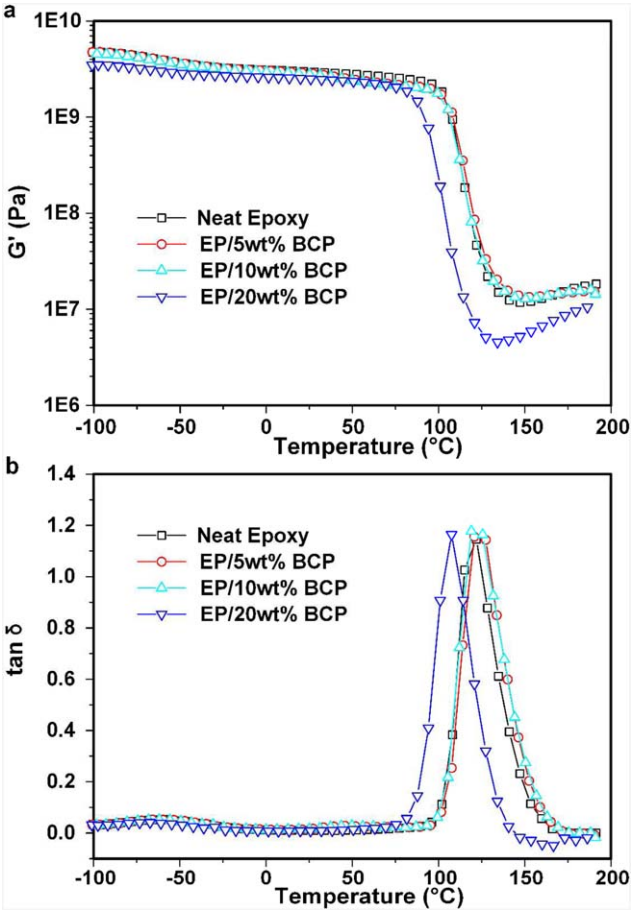

Figure 7. DMA plots of the neat epoxy and epoxy blends (EP) modified with 5, 10, and 20 wt % SMA–SBAS reactive BCP. The G' values and tan δ curves as a function of the temperature are presented. [Color figure can be viewed in the online issue, which is available at wileyonlinelibrary.com.]

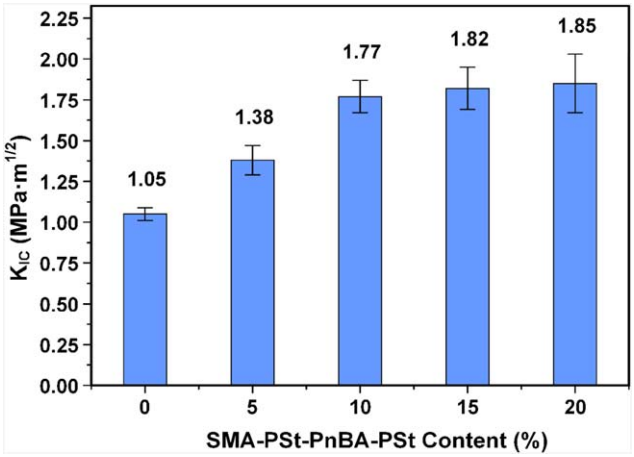

Figure 8. K_{IC} values of various loadings of the SMA–SBAS reactive tetrablock copolymer modified DGEBA/DDM thermosets. [Color figure can be viewed in the online issue, which is available at wileyonlinelibrary.com.]

structures of micrometer voids on the fracture surface observed by SEM.

At higher BCP concentrations, the SMA solubility in the uncured epoxy matrix was not able to disperse individual BCP spherical domains during the cosolvent evaporation process. The irreversible coalescences of these micelles led to larger BCP inclusions. These microdomains were able to scatter visible light. Therefore, the transmittance of blends containing higher BCP concentrations decreased. The transition from microphase separation to macrophase separation with increasing amounts of amphiphilic nonreactive BCPs has also been reported in previous studies.[19] Scheme 3 shows the concept of the different inclusions in the SMA–SBAS modified epoxy blends. The self-assembling property and reactive nature of the reactive tetrablock copolymer produced nanospheres, vesicles, and complex inclusions at different loadings.

DMA

The DMA data obtained from the cured epoxy blends modified by SMA–SBAS are presented in Figure 7. The first T_g around −60°C corresponded to the β transitions of the epoxy network and small fractions of PnBA segments (−45°C for PnBA) of SMA–SBAS.[39] The second T_g corresponded to the α transitions of the epoxy network and small fractions of PSt segments (90°C for PSt). Cured epoxy blends containing 5 wt % SMA–SBAS blends (124°C) and 10 wt % SMA–SBAS blends (121°C) showed a small increase in T_g compared to the cured neat epoxy (120°C). The addition of 10 wt % SMA–SBAS to the epoxy brought about no reduction in the stiffness. However, the 20 wt % SMA–SBAS modified epoxy blends showed a noticeable reduction in G' at all temperatures and a significant reduction in T_g. Samples with both 10 and 20 wt % SMA–SBAS exhibited slightly higher tan δ values between the α and β transitions; this indicated a more ductile matrix at room temperature.[40]

K_{IC}

The K_{IC} values of the cured epoxy blends with different concentrations of SMA–SBAS tetrablock copolymer are compared in Figure 8. In this study, neat epoxy showed a K_{IC} value of about 1 MPa $m^{1/2}$. The K_{IC} of the SMA–SBAS modified blends was higher than that of the unmodified neat epoxy. Cured blends containing 5 and 10 wt % of SMA–SBAS with nanospheres and vesicles imparted 31 and 69% increases in K_{IC}, respectively. However, at high BCP concentrations (15 and 20 wt %), the complex inclusions produced no significant improvements in toughness. Larger particles acted as defects, and this could have resulted in the premature failure of the matrix and, hence, lowered the overall toughness.[41] These defects caused certain drawbacks to the toughness. Therefore, only a slight increase in K_{IC} was observed with the additions of 15 and 20 wt % reactive BCP. We also noted that the K_{IC} values of higher volume fractions of epoxy/SMA–SBAS had noticeably higher standard deviations than the lower load samples. This was probably due to the fact that the native crack tip radius of the epoxy was of the same order as the length of the inclusions on the submicrometer scale. Depending on exactly where the crack tip was located with respect to the macroscopic structure, the resistance against crack propagation varied. In contrast, for epoxies without SMA–SBAS, the location of the crack tip with respect to the micelles became irrelevant. This led to larger deviations in the K_{IC} results of the BCP-modified blends compared to those of the cured neat epoxy. Because the critical stress intensity value of the 10 wt % epoxidized polystyrene-*block*-poly(*n*-butyl acrylate)-*block*-polystyrene in DGEBA/DDM blends was slightly higher than that of the neat epoxy, as reported in literature,[29] the 69% increase in K_{IC} of the 10 wt % SMA–SBAS in the

Table II. K_{IC}, G_{IC}, E, and T_g of the SMA–SBAS-Modified Epoxy Resins investigated in This Study

Sample	K_{IC} (MPa $m^{1/2}$)[a]	E (GPa)[b]	G_{IC} (J/m^2)[c]	T_g (°C)[d]
Neat epoxy	1.05	2.98	327.20	120
5% SMA-SBAS modified blends	1.23	2.87	466.21	124
10% SMA-SBAS modified blends	1.77	2.81	986.03	121
15% SMA-SBAS modified blends	1.82	2.51	1167.13	119
20% SMA-SBAS modified blends	1.85	2.50	1210.74	107

[a] The stress intensity factor (K_{IC}) was obtained from SENB tests on at least five samples.
[b] E was obtained from DMA.
[c] G_{IC} was calculated from K_{IC} and E with $G_{IC} = K_{IC}^2 (1 - \nu^2)/E$, where ν is Poisson's ratio and is equal to 0.34.
[d] T_g values were obtained from DMA.

DGEBA/DDM blends was attributed to the strong interfacial adhesion between reactive BCP and the epoxy matrix.

The mechanical properties of the epoxy blends in this study are presented in Table II. The elastic modulus (E) of the macrophase-separated ones were significantly lower than that of the microphase-separated ones. The low-modulus inclusions were able to reduce the plastic resistance of the epoxy matrix. Similar trends have also been described elsewhere.[17,23] The critical strain energy release rate (G_{IC}) value of the unmodified epoxy resin was 327 J/m^2; meanwhile, K_{IC} of the epoxy blends modified by 5 wt % SMA–SBAS with a nanosphere morphology was about 466 J/m^2. For the 10 wt % SMA–SBAS modified epoxy blend sample, a twofold increase in G_{IC} compared to the unmodified epoxy resin was obtained. For the 5 and 10 wt % SMA–SBAS modified epoxy resins, the cavitation of the sphere micelles and the shear banding of epoxy matrix was likely the major mechanisms in toughening. For the 15 and 20 wt % SMA–SBAS modified epoxy resins, as the inclusion size was more comparable to the plastic zone, and cavitation, crack deflecting, and interfacial bridging were responsible for the improvements in G_{IC}. The detailed toughening mechanisms will be discussed in future studies.

CONCLUSIONS

An SMA–SBAS reactive tetrablock copolymer was used as the reactive toughening modifier for the DGEBA/DDM epoxy resin. By introducing SMA segments into an initially epoxy-immiscible triblock copolymer, the inclusion size was successfully controlled at the submicrometer scale. K_{IC} was improved through the incorporation of a reactive tetrablock copolymer into epoxy matrix. A 69% increase in K_{IC} with nanospheres and a 76% increase in K_{IC} with nanomicrocomplex inclusions relative to the unmodified epoxy resin were achieved. Cured blends with microphase separation showed a slightly increased T_g, whereas complex inclusions brought drawbacks in T_g because of macrophase separation.

ACKNOWLEDGMENTS

The authors thank the National Science Foundation of China (awards 21176212, 21276224, and 21476195) and the Zhejiang Provincial National Science Foundation of China (contract grant number Y14B060038) for supporting this research.

REFERENCES

1. Bascom, W. D.; Cottington, R. L.; Jones, R. L.; Peyser, P. *J. Appl. Polym. Sci.* **1975**, *19*, 2545.
2. Pearson, R. A.; Yee, A. F. *J. Appl. Polym. Sci.* **1993**, *48*, 1051.
3. Sankaran, S.; Chanda, M. *J. Appl. Polym. Sci.* **1990**, *39*, 1635.
4. Zhou, H.; Song, X.; Xu, S. *J. Appl. Polym. Sci.* **2014**, *131*, 41110.
5. Jing, X.; Liu, Y.; Liu, Y.; Liu, Z.; Tan, H. *J. Appl. Polym. Sci.* **2014**, *131*, 40853.
6. Yu, X.; Zhang, C.; Ni, Y.; Zheng, S. *J. Appl. Polym. Sci.* **2013**, *128*, 2829.
7. Ochi, M.; Ichikawa, N.; Harada, M.; Hara, M.; Uchida, H. *J. Appl. Polym. Sci.* **2012**, *124*, 4572.
8. Kuan, H.; Dai, J.; Ma, J. *J. Appl. Polym. Sci.* **2010**, *115*, 3265.
9. Lin, K.; Shieh, Y. *J. Appl. Polym. Sci.* **1998**, *70*, 2313.
10. Yao, D.; Kuila, T.; Sun, K. B.; Kim, N. H.; Lee, J. H. *J. Appl. Polym. Sci.* **2012**, *124*, 2325.
11. Mijovic, J.; Shen, M.; Sy, J. W.; Mondragon, I. *Macromolecules* **2000**, *33*, 5235.
12. Dean, J. M.; Verghese, N. E.; Pham, H. Q.; Bates, F. S. *Macromolecules* **2003**, *36*, 9267.
13. Serrano, E.; Tercjak, A.; Kortaberria, G.; Pomposo, J. A.; Mecerreyes, D.; Zafeiropoulos, N. E.; Stamm, M.; Mondragon, I. *Macromolecules* **2006**, *39*, 2254.
14. Rebizant, V.; Venet, A.; Tournilhac, F.; Girard-Reydet, E.; Navarro, C.; Pascault, J.; Leibler, L. *Macromolecules* **2004**, *37*, 8017.
15. Blanco, M.; López, M.; Kortaberria, G.; Mondragon, I. *Polym. Int.* **2010**, *59*, 523.
16. Cong, H.; Li, L.; Zheng, S. *Polymer* **2014**, *55*, 1190.
17. Wu, J.; Thio, Y. S.; Bates, F. S. *J. Polym. Sci. Part B: Polym. Phys.* **2005**, *43*, 1950.
18. Dean, J. M.; Grubbs, R. B.; Saad, W.; Cook, R. F.; Bates, F. S. *J. Polym. Sci. Part B: Polym. Phys.* **2003**, *41*, 2444.
19. Cano, L.; Builes, D. H.; Tercjak, A. *Polymer* **2014**, *55*, 738.
20. Ruiz-Pérez, L.; Royston, G. J.; Fairclough, J. P. A.; Ryan, A. *J. Polymer* **2008**, *49*, 4475.
21. Ritzenthaler, S.; Court, F.; Girard-Reydet, E.; Leibler, L.; Pascault, J. P. *Macromolecules* **2002**, *36*, 118.
22. Hydro, R. M.; Pearson, R. A. *J. Polym. Sci. Part B: Polym. Phys.* **2007**, *45*, 1470.
23. Kishi, H.; Kunimitsu, Y.; Imade, J.; Oshita, S.; Morishita, Y.; Asada, M. *Polymer* **2011**, *52*, 760.
24. Chong, H. M.; Taylor, A. C. *J. Mater. Sci.* **2013**, *48*, 6762.
25. Bashar, M. T.; Sundararaj, U.; Mertiny, P. *Polym. Eng. Sci.* **2014**, *54*, 1047.
26. Chen, J.; Taylor, A. C. *J. Mater. Sci.* **2012**, *47*, 4546.
27. Grubbs, R. B.; Dean, J. M.; Broz, M. E.; Bates, F. S. *Macromolecules* **2000**, *33*, 9522.
28. George, S. M.; Puglia, D.; Kenny, J. M.; Jyotishkumar, P.; Thomas, S. *Polym. Eng. Sci.* **2012**, *52*, 2336.
29. George, S. M.; Puglia, D.; Kenny, J. M.; Causin, V.; Parameswaranpillai, J.; Thomas, S. *Ind. Eng. Chem. Res.* **2013**, *52*, 9121.
30. George, S. M.; Puglia, D.; Kenny, J. M.; Parameswaranpillai, J.; Thomas, S. *Ind. Eng. Chem. Res.* **2014**, *53*, 6941.
31. Grubbs, R. B.; Dean, J. M.; Bates, F. S. *Macromolecules* **2001**, *34*, 8593.
32. Rebizant, V.; Abetz, V.; Tournilhac, F.; Court, F.; Leibler, L. *Macromolecules* **2003**, *36*, 9889.
33. Bowes, A.; Mcleary, J. B.; Sanderson, R. D. *J. Polym. Sci. Part A: Polym. Chem.* **2007**, *45*, 588.
34. Zetterlund, P. B.; Kagawa, Y.; Okubo, M. *Chem. Rev.* **2008**, *108*, 3747.

35. Liang, G.; Meng, J.; Zhao, L. *Polym. Int.* **2003**, *52*, 966.
36. Zhan, X.; He, R.; Zhang, Q.; Chen, F. *RSC Adv.* **2014**, *4*, 51201.
37. Ritzenthaler, S.; Court, F.; David, L.; Girard-Reydet, E.; Leibler, L.; Pascault, J. P. *Macromolecules* **2002**, *35*, 6245.
38. Kishi, H.; Kunimitsu, Y.; Imade, J.; Oshita, S.; Morishita, Y.; Asada, M. *Polymer* **2011**, *52*, 760.
39. Luo, Y.; Wang, X.; Zhu, Y.; Li, B.; Zhu, S. *Macromolecules* **2010**, *43*, 7472.
40. Liu, J. D.; Thompson, Z. J.; Sue, H.; Bates, F. S.; Hillmyer, M. A.; Dettloff, M.; Jacob, G.; Verghese, N.; Pham, H. *Macromolecules* **2010**, *43*, 7238.
41. Thio, Y. S.; Wu, J.; Bates, F. S. *J. Polym. Sci. Part B: Polym. Phys.* **2009**, *47*, 1125.